New mechanism, new chromophore: investigating the electrophilic behaviour of styrylindolium dyes

Alexis Perry[a*]
a – Biosciences, University of Exeter, Stocker Road, Exeter EX4 4QD, UK.
* – A.Perry@Exeter.ac.uk

Introduction

Styrylindolium dyes (e.g. **1**-**5**, Figure 1) are a common class of merocyanine, widely used in sensing and imaging and frequently encountered as the coloured, ionic isomer of a spiropyran-merocyanine pair.[1–6] Styrylindolium cations possess extended π-conjugation and hence display visible absorbance (~400 nm) and fluorescence emission (~600 nm),[7] and their central conjugated iminium ion is a competent electrophile. Nucleophilic attack upon this π-system will inherently alter its optical properties, therefore styrylindolium species are employed as colourimetric and fluorimetric receptors for nucleophilic analytes. In this role, the styrylindolium core has been exploited as the reactive component within sensors for biologically and environmentally important nucleophiles such as cyanide,[8–20] sulfide,[21–25] bisulfite,[26–28] fluoride[20] and sulfur-containing amino acids,[29–31] and this approach has been successfully validated in live cells[18,21,24,27,28,31] and in specific organelles.[22] FRET-based ratiometric probes (e.g. **3**,[23] **4**[15] and **5**[26]) have been developed through conjugation of styrylindolium cations to complementary fluorophores, and novel hybrid materials have incorporated styrylindolium units within polymer and nanoparticle structures.[11,13,24]

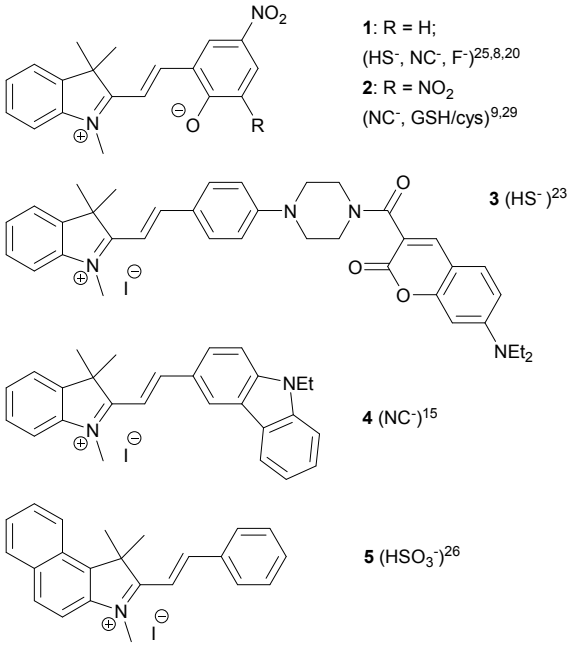

Figure 1 – Styrylindolium-based sensors used for nucleophilic analytes (respective analytes in parentheses)

As alluded to above, nucleophilic attack upon the dye structure results in modification of its chromophore, hence providing a quantifiable output; therefore, it is important that all interactions between dye and nucleophile are

well characterised such that sensor behaviour can be fully understood. Nucleophilic addition to the styrylindolium core commonly occurs by 1,2- or 1,4-attack on the unsaturated iminium ion; or, alternatively, the presence of conjugated electron withdrawing substituents on the styryl ring can promote attack at the opposite end of the alkene (Scheme 1).[30] An extra layer of complexity can also be encountered through reduction of susceptible functional groups by analytes such as sulfide[32] and the formation of per/polysulfide products in the presence of sulfur-centred nucleophiles.[33]

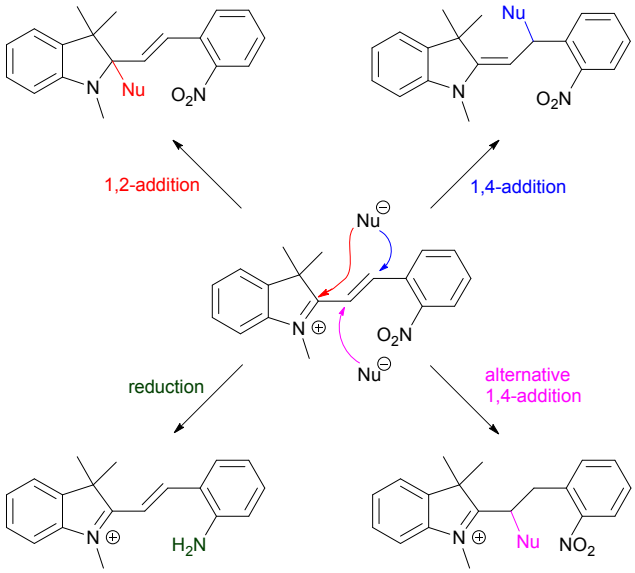

Scheme 1 – Potential reaction pathways for a nucleophile with a nitrosubstituted styrylindolium cation

Given these numerous, potentially competitive reaction pathways and the structural complexity of many styrylindolium-based sensors, full mechanistic characterisation of sensor–nucleophile interactions is challenging. Although several publications exhibit admirably comprehensive analysis,[10,20,24] this is by no means general or indeed possible in every case. Furthermore, compounds such as **1** and **2** have been claimed as highly selective probes for several different, apparently competitive analytes under similar conditions, and it is apparent that clarity would benefit this field significantly.

In order to untangle this somewhat confused picture, the aim of this study was to assess the reactivity of simple styrylindolium dyes towards a range of relevant nucleophiles, hence providing a basis upon which to understand the behaviour of more complex styrylindolium systems. This work does not present encyclopaedic coverage; rather, we have selected model indolium structures and analytes to represent what is commonly present in practice and to provide a clear view of the stereoelectronic effects which govern nucleophilic addition. The styrylindolium substituents and substituent patterns were chosen to cover both electron withdrawing (inductive and mesomeric) and donating substituents, both in and out of conjugation with the iminium ion and with their electronic effects opposed; and a further example which mirrors the substituent pattern of the common spiropyran-merocyanine nitrobips **1** but

lacks the complexity presented by this compound's *spiro-mero* isomerism (Scheme 2). The nucleophiles included in this study encompass common analytes for styrylindolium cations ($^{-}$CN, $^{-}$SH), and methanethiolate was employed as a simple model nucleophile for sulfur-based analytes (e.g. thiol-containing amino acids). It is envisaged that the trends in reactivity that are identified herein will inform the future design of styrylindolium-based sensors.

Results and Discussion

Synthesis of styrylindolium iodides **7a**-**g** was achieved through condensation of 1,2,3,3-tetramethylindolium iodide (**6**) with appropriate benzaldehydes (Scheme 2). Whilst published methods offer a variety of conditions with which to promote such reactions,[34–40] the protocol of Metsov, Dudev and Koleva, employing refluxing acetic acid, proved to be the most straightforward and effective for all substrates.[34] Using these conditions, iodides **7a**-**g** were obtained in varied yield.

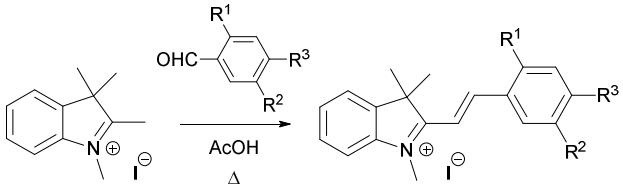

6

7a; $R^1 = R^2 = R^3 = H$; 37%
7b; $R^1 = R^2 = H$, $R^3 = OMe$; 80%
7c; $R^1 = R^2 = H$, $R^3 = Br$; 55%
7d; $R^1 = OMe$, $R^2 = NO_2$, $R^3 = H$; 30%
7e; $R^1 = R^3 = H$, $R^2 = NO_2$; 51%
7f; $R^1 = R^2 = H$, $R^3 = NO_2$; 83%
7g; $R^1 = OMe$, $R^2 = H$, $R^3 = NO_2$; 43%

Scheme 2 – Synthesis of styrylindolium iodides **7a**-**g**

With styrylindolium salts **7a**-**g** in hand, we exposed each salt to tetrabutyl ammonium cyanide, sodium sulfide and sodium methanethiolate, and carefully analysed the products of each reaction. Primarily, this analysis employed NMR techniques (^{1}H, ^{13}C, COSY, HSQC, HMBC and NOESY) which enabled connectivity between the nucleophile and its specific site of attachment to the substrate to be established. ESI mass spectrometry and UV-vis spectroscopy were employed as necessary to provide clarification where NMR analysis proved ambiguous (e.g. in identification of nitro to amine reduction.)

Reactions between styrylindolium cations and cyanide, sulfide or thiolate are often rapid (<1 min) at room temperature and occur readily in non-degassed, non-dried solvents under a non-inert atmosphere. Given the robust nature of these reactions, and with the use of NMR as our primary analytical tool, reactions were conducted in DMSO-d_6, using standard NMR tubes as reaction vessels. In order to deconvolute the products of competing reaction pathways, and to appreciate the relative rates of these processes, nucleophiles were added in 0.5 eq. increments (up to 5 eq. total), with spectroscopic analysis taking place following each addition.

To illustrate this approach, Figures 2 and 3 demonstrate the key spectra used to elucidate the products of the reactions between 4-bromo salt **7c** and $^{-}$CN,

$^{-}$SMe and $^{-}$SH. Reaction of cyanide with **7c** proceeded with near-exclusive1,2-attack upon the iminium ion to give adduct **8c**. ^{1}H NMR illustrates loss of the deshielding influence of the positively charged nitrogen atom with general upfield shifts of the unsaturated protons and a 1.5 ppm upfield shift of the NMe group (Figure 2a), and this is consistent with published results in related compounds.[8,15] 1,4-Addition can be discounted given that the *trans*-alkene remains intact (16.5 Hz in **7c**; 16.1 Hz in **8c**) and that no new aliphatic protons can be identified. Critically, HMBC analysis (Figure 2b) allows connectivity between the cyanide carbon atom and alkene proton to be established (as the sole correlation for CN), unambiguously identifying the site of nucleophilic addition.

In contrast, methanethiolate addition to **7c,** whilst also a relatively clean process, proceeded by 1,4 attack upon the styrylindolium electrophile to produce adduct **9c** as a 7:3 mixture of *E* and *Z* isomers. As with cyanide addition, loss of the iminium ion is accompanied by a general upfield migration of proton resonances. Adduct **9c** contains adjacent methine and enamine protons and these produce a prominent AB pattern between 4 and 5 ppm (***E*-9c**, J = 11.2 Hz; ***Z*-9c**, J = 10.2 Hz). Attachment of the SMe group to the methine carbon is evident through HMBC analysis, wherein correlation between the SMe protons and the methine C atom can be identified (Figure 2b), and *E* / *Z* configurations have been determined by identification of through-space interactions between the alkene proton and NCH_3 (*E*-isomer) or $C(CH_3)_2$ (*Z*-isomer)(see ESI). Given the absence of published data to compare with these somewhat complex NMR spectra (^{1}H NMR spectra have been published documenting apparent 1,4-addition of bisulfite to styrylindolium species [26], but these do not correspond closely to our observations), we further confirmed the identity of **9c** through ESI mass spectrometry: parent ions M+ were observed at m/z = 387/389 (reflecting bromine isotopes) and fragments corresponding to loss of SMe were apparent (m/z = 340/342)(Figure 3, top).

In contrast, sulfide addition to **7c** was not a clear-cut process and this was reflected by its complex ^{1}H NMR spectrum, consisting of at least 4 major components (Figure 2a). Despite this confused picture, the spectrum does contain methine / enamine peaks characteristic of 1,4-addition (comparable with those of **9c**) and given the absence of any reducible functional groups, the complete consumption of starting material and the lack of *trans* alkene protons, 1,4 attack followed by polysulfide formation may provide a plausible explanation (1,4-addition–protonation–1,2-addition may provide an additional pathway though this is disfavoured under basic conditions). The corresponding mass spectrum of this reaction mixture was surprisingly clear, with m/z = 340/342 and 262 suggesting loss of SH then subsequent loss of Br (Figure 3, bottom). The absence of heavier ions perhaps reflects the instability of polysulfide species in electrospray ionisation.

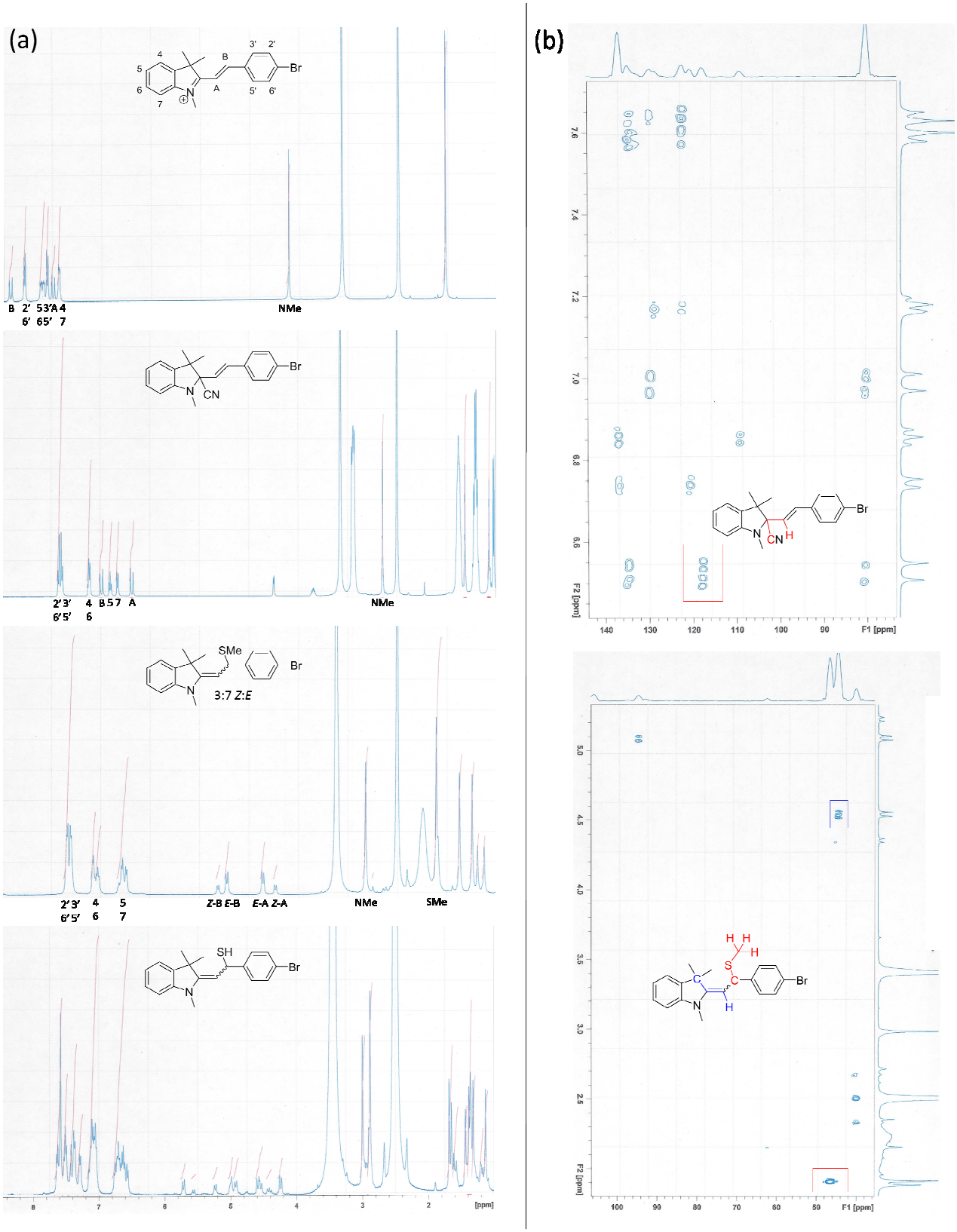

Figure 2 – Reactions of 4-bromostyrylinolium iodide **7c** with nucleophiles (3 eq.) in DMSO-d_6 (a) ^{1}H NMR spectra, top to bottom: **7c**; **7c** + $(Bu_4N)CN$; **7c** + NaSMe; **7c** + $Na_2S{\cdot}9H_2O$. (b) HMBC spectra showing key correlations for (top) cyanide and (bottom) methanethiolate addition.

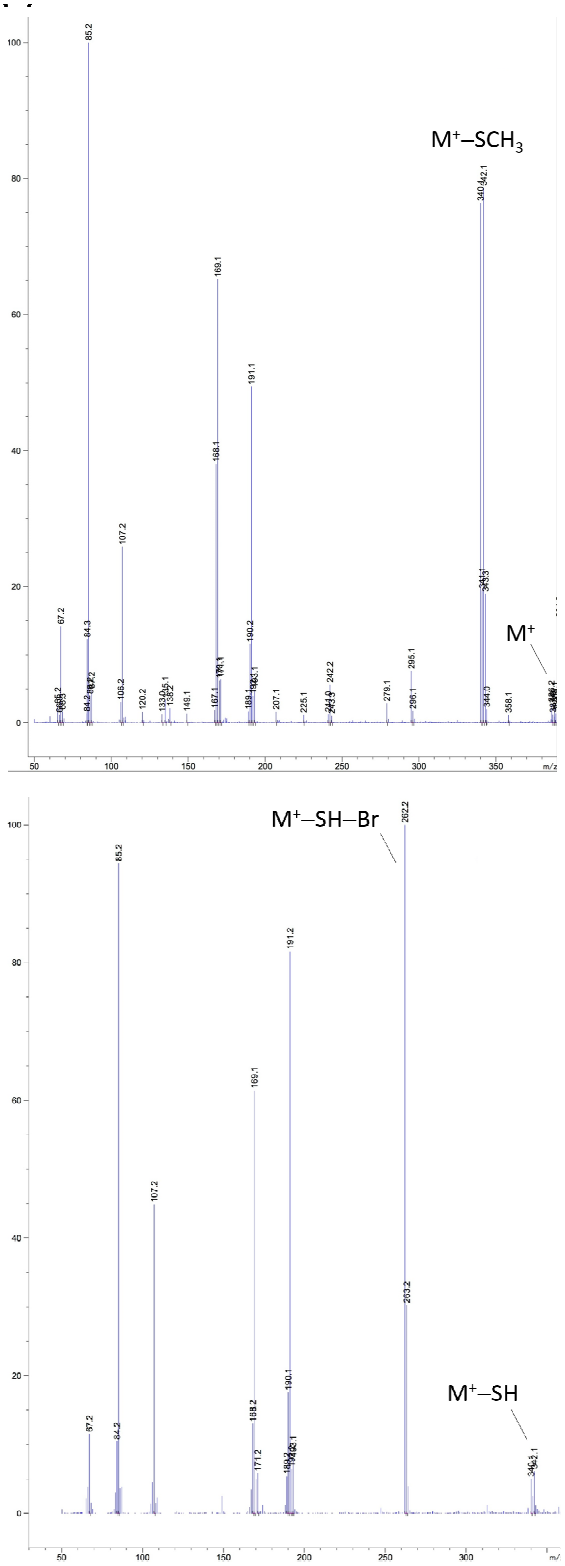

Figure 3 – Reactions of 4-bromostyrylinolium iodide **7c** with nucleophiles (3 eq.) in DMSO-d_6. Mass spectra for (top) methanethiolate and (bottom) sulfide addition.

Similar analyses were applied to styrylindolium iodides **7a**-**g**, the results of which are summarised in Scheme 3 and Table 1, and all relevant spectra are available in supporting information. In brief, cyanide reacted very cleanly with all seven styrylindolium iodides to give the products of 1,2-addition, **8a**-**g**; methanethiolate reacted in general by clean 1,4-addition to give adducts **9a**-**e** as mixtures of *E* and *Z* alkenes; whereas sulfide displayed a tendency to give complex mixtures of products, in which initial 1,4-addition was succeeded by presumed polysulfide formation. For compounds **7d** and **e** (entries 4 and 5), addition of excess sulfide resulted in reduction of aromatic nitro groups to anilines **10h** and **i** (as evidenced by mass spectrometry) and similar but slower reduction was observed with excess methanethiolate to give the aniline products **9h** and **i**.

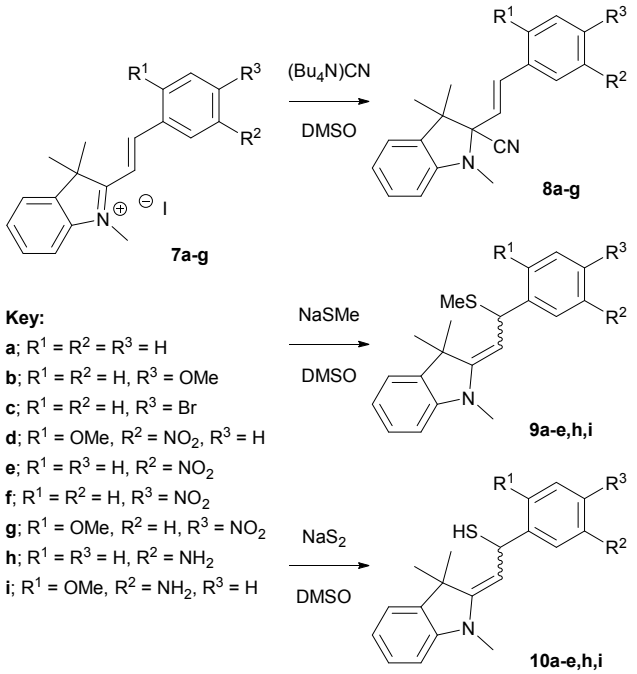

Scheme 3 – Reactions of styrylindolium salts **7** with cyanide, methanethiolate and sulfide

Table 1 – Summary of major reaction pathways and products from reaction of styrylindolium salts **7** with cyanide, methanethiolate and sulfide

Entry	Indolium iodide	Reaction with $^{-}$CN (products)	Reaction with $^{-}$SMe (products)	Reaction with $^{-}$SH (products)
1	**7a**	1,2-addition (**8a**)	1,4-addition (**9a**; *Z*:*E* 29:71)	1,4-addition (**10a**) and polysulfidation
2	**7b**	1,2-addition (**8b**)	1,4-addition (**9b**; *Z*:*E* 24:76)	1,4-addition (**10b**) and polysulfidation
3	**7c**	1,2-addition (**8c**)	1,4-addition (**9c**; *Z*:*E* 29:71)	1,4-addition (**10c**) and polysulfidation
4	**7d**	1,2-addition (**8d**)	1,4-addition (**9d**) and reduction (**9i**;	1,4-addition (**10d**) reduction (**10i**)

			Z:*E* 9:91)	and polysulfidation
5	**7e**	1,2-addition (**8e**)	1,4-addition (**9e**; *Z*:*E* 15:85) and reduction (**9h**)	1,4-addition (**10e**) reduction (**10h**) and polysulfidation
6	**7f**	1,2-addition (**8f**)	1,8-addition (**11a**)	1,8-addition (**11b**)
7	**7g**	1,2-addition (**8g**)	1,8-addition (**11c**)	Unclear

The distribution of electron density in styrylindolium species is complex, though, as a general trend, electron-releasing styryl substituents favour polymethine-type structures with greater conjugation and bond equalisation, whereas electron-withdrawing substituents confer greater polyene character.[7,34] In light of this, it is perhaps surprising that little difference in reactivity was noted across the styrylindolium substrates included in this study. We explain the observed regioselectivity on the basis of standard hard/soft interactions, wherein attack on the charged iminium ion is favoured by harder nucleophiles and conjugate addition to the alkene is favoured by softer nucleophiles. It is important to note that although cyanide attack occurs at the iminium ion, it is not a classical hard nucleophile (HCN: pK_a = 9.2; H_2O: pK_a = 14.0; H_2S = 7; chemical hardness (eV), $^-$CN: η = 5.3; $^-$OH: η = 5.6; $^-$SH: η = 4.1),[41] hence the conjugate addition pathway is accessible only to particularly soft nucleophiles. We saw no evidence of nucleophilic addition to the α-carbon of the iminium ion (contrary to that reported by Li *et al*)[30] and, regardless of the electronics of the styrylindolium ion and the regioselectivity of addition, nucleophilic attack was always rapid and would always consume the substrate.

A fascinating and potentially important result was observed in an exception to this general pattern of reactivity. Addition of excess sodium methanethiolate to *p*-nitro compound **7f** resulted in rapid formation of a dark purple solution (1,2- and 1,4-addition cause merocyanine decolourisation by breaking extended conjugation) and analysis of this solution by ^{1}H NMR showed a clean spectrum corresponding to the presumed product of 1,8-addition, **(*E*)-11a**, as a single geometric isomer (Scheme 4). Given the scarcity of examples of 1,8-addition generally[42,43] and the absence of examples within merocyanine chemistry, we undertook careful and thorough analysis to confirm this structure. Data from mass spectrometry supported the identity of **11a** as an adduct of mono-SMe addition (m/z = 354 (M^+)). Key evidence for **11a** was apparent in its ^{1}H NMR spectrum: general upfield migration of resonances implied loss of the deshielding indolium cation; disruption of the *trans*-alkene ($^3J_{AB}$ = 16.5 Hz in **7f**; 13.2 Hz in **11a**) and the absence of new aliphatic proton resonances are inconsistent with 1,2- and 1,4-addition respectively; and appearance of two AB patterns (6.95/6.56 ppm: 9.9 Hz; 6.70/6.17 ppm; 10.1 Hz) implies formation of two *cis*-alkenes (Figures 4a and 4b). Through-bond and through-space correlations, identified by COSY/HMBC and NOESY experiments, supported the proposed structure in general and crucially enabled the connectivity between the SCH_3 group and the main framework to be established (Figure 4c). The reactivity of **7f** with sulfide was similar to that observed with methanethiolate; however, in this case, initial 1,4-addition

preceded equilibration (<1 h) to the 1,8-adduct **(*E*)-11b** in near-exclusivity. We found no evidence for nitro group reduction of **11a** or **11b**, and this is consistent with structures possessing aliphatic nitro groups, given that such nitro groups are considerably less reactive towards sulfide reduction than nitrobenzene derivatives.[44]
Analogous 1,8-addition of methanethiolate to 2-methoxy-4-nitro compound **7g** gave **(*E*,*E*)-11c** as a single geometric isomer (Scheme 4), demonstrating that 4-nitrostyrylindolium salts will undergo 1,8-addition with methanethiolate as their principal mechanism regardless of apparently opposing electronic effects. On the other hand, in the corresponding reaction of **7g** and sulfide, the dominance of the 1,8-addition pathway was blunted by the electron-donating character of the methoxy substituent; in this case, initial 1,4-addition preceded formation of a complex mixture of products.

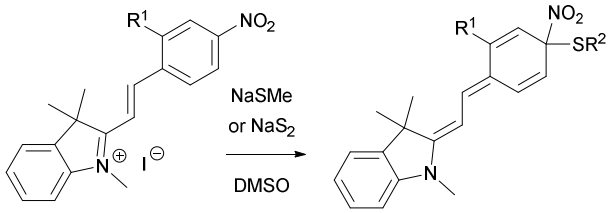

7f; R^1 = H
7g; R^1 = OMe

11a; R^1 = H, R^2 = Me
11b; R^1 = H, R^2 = H
11c; R^1 = OMe, R^2 = Me

Scheme 4 – Reaction of p-nitrostyrylindolium salts **7f** and **g** with methanethiolate and sulfide

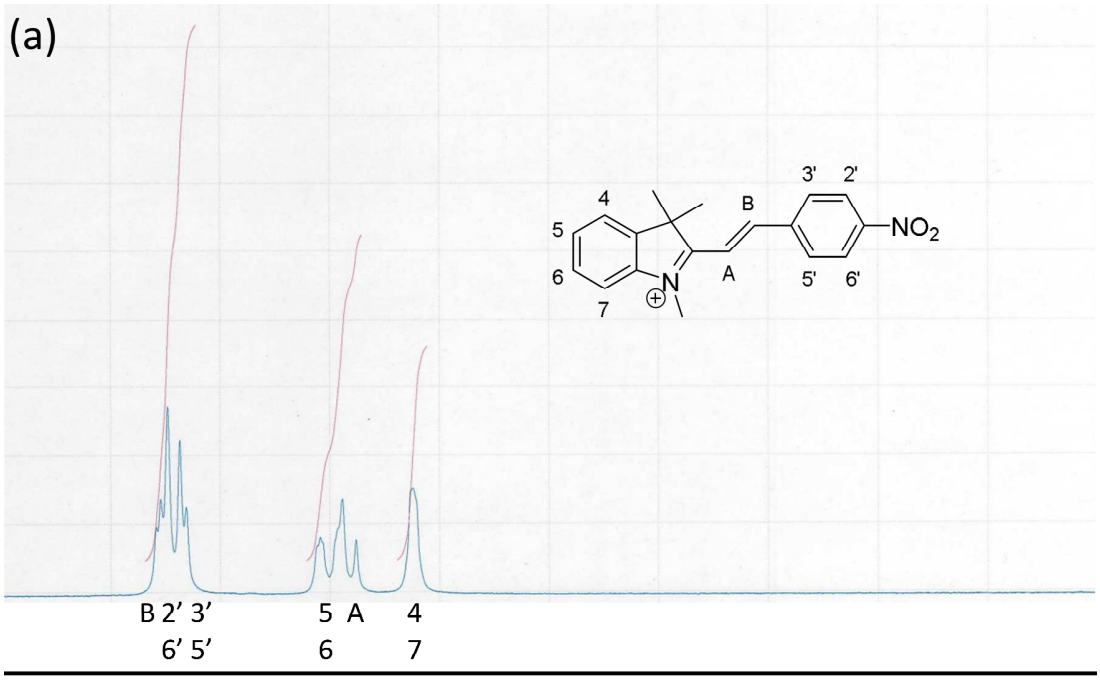
(a)
B 2’ 3’
6’ 5’
5 A
6
4
7
4
5
6
7
N
B
A
3' 2'
5' 6'
NO2

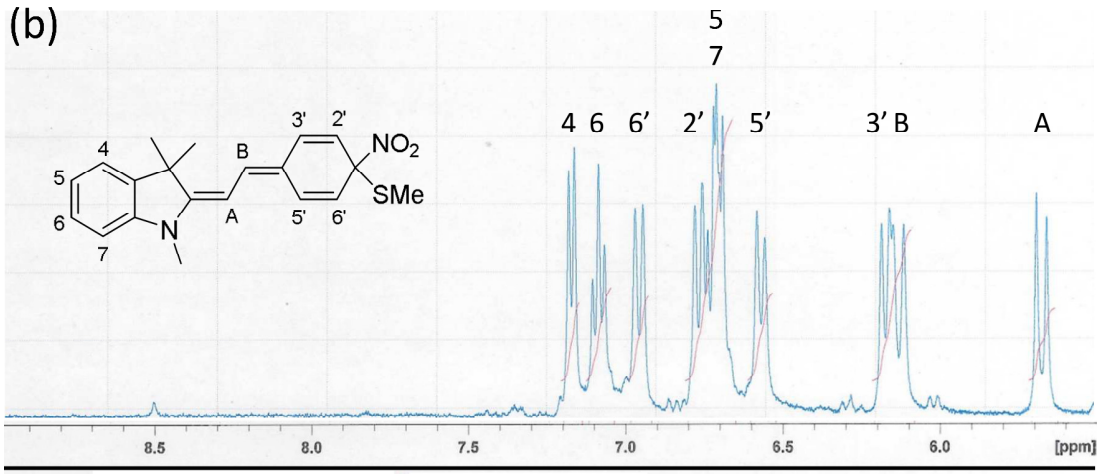
(b)
5
7
4 6 6’ 2’ 5’ 3’ B A
4
5
6
7
N
B
A
3' 2'
5' 6'
NO2
SMe
8.5
8.0
7.5
7.0
6.5
6.0
[ppm]

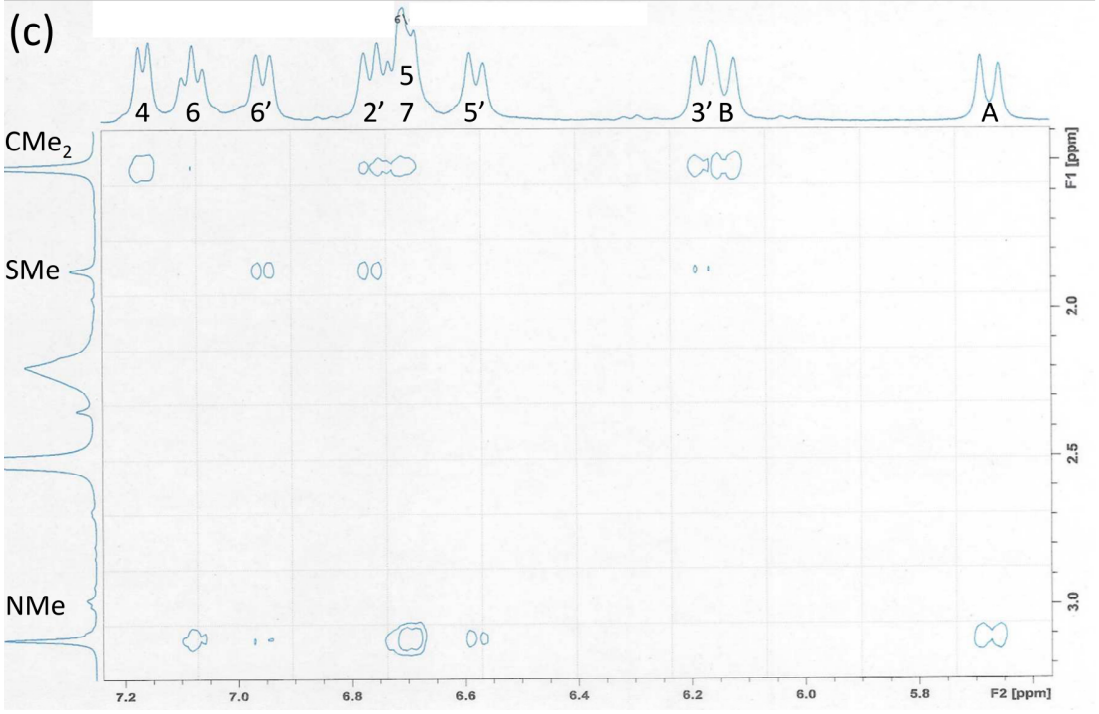
(c)
4 6 6’ 2’ 5 7 5’ 3’ B A
CMe2
SMe
NMe
F1 [ppm]
2.0
2.5
3.0
7.2
7.0
6.8
6.6
6.4
6.2
6.0
5.8
F2 [ppm]

Figure 4 – 1,8-Addition of methanethiolate to 4-nitrostyrylindolium iodide **7f**. (a) and (b): Expansion of aromatic region of ^{1}H NMR spectrum for **7f** and for **7f** + NaSMe (3 eq.) (c) NOESY spectrum for **7f** + NaSMe, illustrating key correlations between SMe and 2′/6′ protons.

The extended conjugation of **11a** and **11b** is consistent with their intense colouration and, given the application of styrylindolium dyes in sensing, the optical properties of **7f** were quantified by UV-visible spectroscopy (Figure 5a) and fluorescence spectroscopy. Merocyanine **7f** in DMSO solution appears yellow and correspondingly displays a strong absorbance at 390 nm (Figure 5a; blue line). Following addition of NaSMe, this band is rapidly eroded, with concomitant appearance of a red-shifted absorbance at 550 nm consistent with formation of **11a** (yellow line). A similar effect was observed following the addition of sulfide to **7f**, reflecting the formation of 1,8-adduct **11b** (orange line). For comparison, analogous analyses followed the reactions of **7f** with cyanide (Figure 5a, green line), and *p*-methoxystyryl derivative **7b** with cyanide, methanethiolate and sulfide (Figure 5b). In each case, products displayed blue-shifted absorbance maxima, implying loss of extended conjugation, consistent with formation of 1,2- and 1,4-adducts **8f**, **8b, 9b** and **10b** respectively. Analysis of 1,8-adduct **11a** in DMSO solution by fluorescence spectroscopy indicated that this compound does not exhibit fluorescence emission. Correspondingly, this 1,8-addition pathway may be exploited within FRET-based sensors, analogous to those employing alternative nucleophilic addition mechanisms to styrylindolium cations (see Introduction and Figure 1 for examples of this approach).

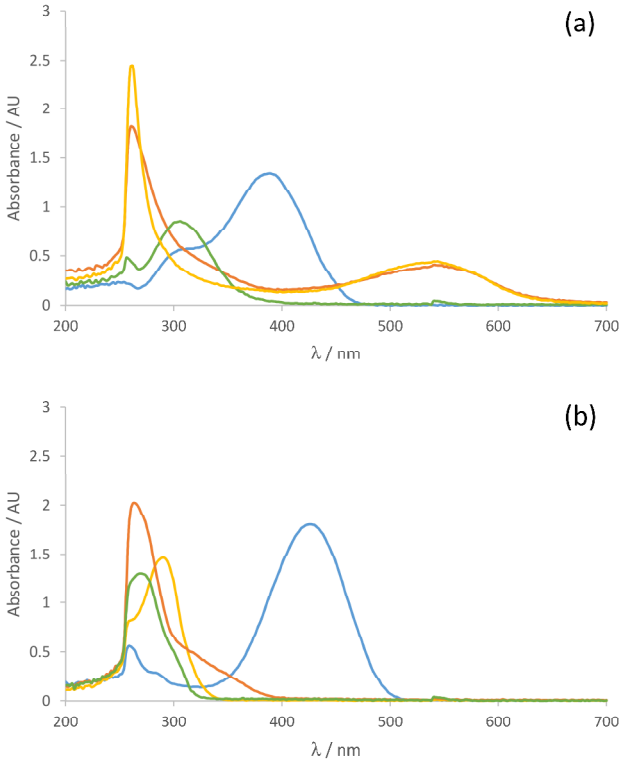

Figure 5 – UV-visible absorbance spectra illustrating addition of nucleophiles to *p*-nitrostyrylindolium salt **7f** (Figure 5a) and *p*-methoxystyrylindolium salt **7b**

(figure 5b). Blue line = **7b**/**7f** (0.0498 mM in DMSO); green line = **7b**/**7f** + Bu_4NCN (10 eq.); yellow line = **7b**/**7f** + NaSMe (10 eq.); orange line = **7b**/**7f** + $Na_2S{\cdot}9H_2O$ (10 eq.).

At first sight, the proposed 1,8-addition seems somewhat implausible given its inherent disruption of styryl aromaticity and the availability of a competing "normal" 1,4-addition pathway lacking such an energetic penalty. With respect to the former point, we surmise that given the documented reduced aromatic character of 4-nitrostyrylindolium salts,[7,34] the barrier to disruption of aromaticity is lowered and this, in combination with the localised effect of the nitro group, serves to lower the ζ-carbon LUMO energy to favour 1,8-attack. In terms of the latter consideration, the α,β-unsaturated iminium ion of **7f** is conjugated to the styryl nitro group and hence the energy of the β-carbon LUMO is raised, disfavouring 1,4-addition. To understand these mechanistic considerations in greater depth, and to explore the influence of substituents upon styrylindolium electronic configuration, density functional theory (DFT) was used. The APFD functional and 6-311+G(2d,p) basis set, plus SMD "universal" modelling for solvation in DMSO, were implemented using Gaussian 16 computational software,[45] to calculate the LUMO of the energy-optimised structure for both the 4-methoxy- and 4-nitrostyrylindolium cations **7b** and **7f**, respectively (Figure 6). In the case of **7b**, the largest calculated LUMO coefficients are consistent with the experimentally observed 1,2- and 1,4-nucleophilic addition exhibited by this compound (Figure 6a). A contrasting picture is predicted for **7f**, however, with the LUMO coefficients associated with the sites of 1,2-, 1,4- and 1,8-addition being of similar magnitude (Figure 6b). Therefore, although the regioselectivity of nucleophilic addition to **7f** is unlikely to be clear-cut, 1,8-addition is certainly plausible. This is consistent with the empirically observed reactivity of **7f** towards sulfur-centred nucleophiles, wherein 1,8-addition predominates and 1,4-addition is evident as a competing process.

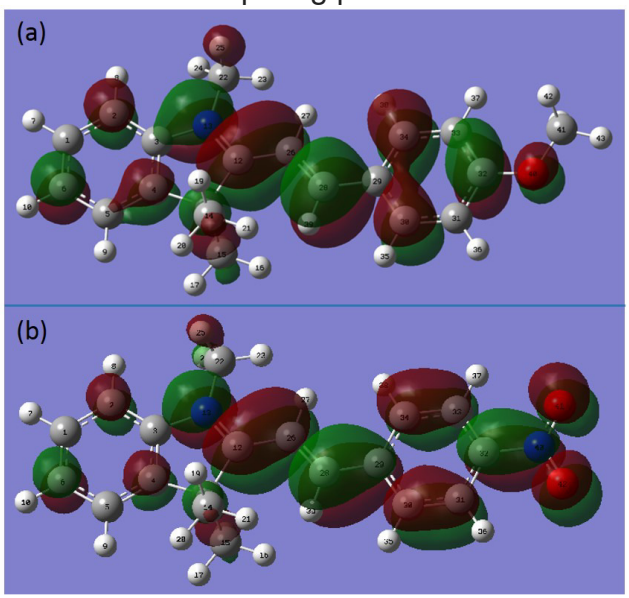

Figure 6 – Optimised structures and visualisations of the LUMO for (a) **7b** and (b) **7f**, based on DFT, ground-state optimisation and frequency calculations.

Conclusions

The aims of this study were to clarify a somewhat confused facet of sensing science and to provide a foundation for the future design of styrylindolium sensors based on empirical observations. Consequently, spectroscopic analysis of reactions between simple model styrylindolium salts and common nucleophilic analytes was conducted, and this enabled patterns of reactivity to be identified which may inform appropriate use and design of this class of sensor molecule. In brief: cyanide undergoes 1,2-addition to the styrylindolium iminium ion; sulfur-based nucleophiles follow a 1,4-addition pathway; persulfide formation is probable in the presence of excess sulfide; nitro groups will be reduced in the presence of excess thiol.

Assuming that optimal sensor behaviour involves clean, high-yielding interaction between sensor and analyte, the inclusion of reducible functional groups within sensors for thiols, or for use within reducing environments, is questionable. This is particularly germane to spiropyran-based probes (e.g. **1** and **2,** Figure 1), wherein nitro groups are commonly employed to provide stabilisation of the merocyanine isomer.[46] The evidence presented here suggests that such probes will undergo divergent reaction pathways when exposed to thiol-based analytes, and that alternative methods of merocyanine stabilisation may be appropriate in these cases.

The key result identified in this study is that *p*-nitrostyrylindolium salts will undergo clean 1,8-addition with sulfur-based nucleophiles, without competitive reduction. To the best of my knowledge, 1,8-nucleophilic addition to merocyanines is undocumented and the conjugated enamine triene structures of **11a-c** represent novel chromophores. The unusual reactivity displayed by **7f** and **g** presents an opportunity to develop a new class of styrylindolium-based sensor for soft nucleophile analytes. Furthermore, **7f** and **g** react *via* clean, complementary pathways with cyanide on one hand and thiols on the other, and this leads to products with very distinct optical characteristics (e.g. **8f**, λ = 306 nm; **11a**, λ = 502 nm). Cyanide and sulfide are often competitive nucleophiles, or, in the case of many styrylindolium salts, react *via* different mechanisms but produce adducts with optical similarity (e.g. **8b**, λ = 270 nm; **9b**, λ = 290 nm, Figure 5b); consequently, the *p*-nitrostyrylindolium core shows ideal characteristics for distinguishing these analytes and may provide the basis for dual-mode sensors.[47] Finally, the reaction in itself possesses synthetic utility, in that such 1,8-additions are rare and the 1,8-adducts are unusual, complex structures with potentially interesting reactivity. Exploration of the scope of this process beyond the indolium core and with alternative nucleophiles and electron-withdrawing groups should reveal some fascinating chemistry.

Conflicts of interest

There are no conflicts to declare.

Acknowledgements

I would like to thank Dr. Debbie Salmon (Mass Spectrometry, University of Exeter) for recording mass spectra of novel compounds presented in this work, Dr. Stephen Green for expertise in modelling studies, and Dr. Mark Wood for insightful discussions.

This research did not receive any specific grant from funding agencies in the public, commercial, or not-for-profit sectors.

References

1. A. V. Kulinich and A. A. Ishchenko, Merocyanine dyes: synthesis, structure, properties and applications, *Russ. Chem. Rev.*, 2009, **78**, 141–164.
2. Y. Hirshberg and E. Fischer, Photochromism and reversible multiple internal transitions in some spiropyrans at low temperatures, *J. Chem. Soc.*, 1954, **0**, 297–303.
3. H. Xia, K. Xie, G. Zou, Advances in Spiropyrans/Spirooxazines and Applications Based on Fluorescence Resonance Energy Transfer (FRET) with Fluorescent Materials, *Molecules*, 2017, **22**, 2236–2252.
4. R. Klajn, *Chem. Soc. Rev.*, 2014, **43**, 148–184.
5. J. Gu, U. Rao, A. Fabio, L. Monte, T. Kramer, R. Heyny von Haußen, J. Hölzer, V. Goetschy-Meyer, G. Mall, I. Hilger, C. Czech and B. Schmidt, 2-Styrylindolium based fluorescent probes visualize neurofibrillary tangles in Alzheimer's disease, *Bioorg. Med. Chem. Lett.*, 2012, **22**, 7667–7671.
6. Y. Li, F. Wei, Y. Lu, S. He, L. Zhao and X. Zeng, Novel mercury sensor based on water soluble styrylindolium dye, *Dyes Pigm.*, 2013, **96**, 424–429.
7. S. Metsov, D. Simov, S. Stoyanov and P. Nikolov, Photophysical characteristics of some 2-styrylindolium dyes, *Dyes Pigm.*, 1990, **13**, 11–19.
8. Y. Shiraishi, K. Adachi, M. Itoh and T. Hirai, Spiropyran as a Selective, Sensitive, and Reproducible Cyanide Anion Receptor, *Org. Lett.*, 2009, **11**, 3482–3485.
9. Y. Shiraishi, M. Itoh and T. Hirai, Rapid colorimetric sensing of cyanide anion in aqueous media with a spiropyran derivative containing a dinitrophenolate moiety, *Tetrahedron Lett.*, 2011, **52**, 1515–1519.
10. S. Sumiya, T. Doi, Y.Shiraishi and T. Hirai, Colorimetric sensing of cyanide anion in aqueous media with a fluorescein–spiropyran conjugate, *Tetrahedron*, 2012, **68**, 690–696.
11. Y. Shiraishi, S. Sumiya, K. Manabe and T. Hirai, Thermoresponsive Copolymer Containing a Coumarin–Spiropyran Conjugate: Reusable Fluorescent Sensor for Cyanide Anion Detection in Water, *ACS Appl. Mater. Interfaces*, 2011, **3**, 4649–4656.
12. Y. Shiraishi, S. Sumiya and T. Hirai, *Chem. Commun.*, 2011, **47**, 4953–4955.
13. H. Xia, J. Li, G. Zou, Q. Zhang and C. Jia, A highly sensitive and reusable cyanide anion sensor based on spiropyran functionalized polydiacetylene vesicular receptors, *J. Mater. Chem. A*, 2013, **1**, 10713–10719.
14. Y. Wang and S. -H. Kim, Colorimetric chemodosimeter for cyanide detection based on spiropyran derivative and its thermodynamic studies, *Dyes Pigm.*, 2014, **102**, 228–233.
15. S. Wang, X. Feia, J. Guoa, Q. Yanga, Y. Lia and Y. Song, A novel reaction-based colorimetric and ratiometric fluorescent sensor for cyanide anion with a large emission shift and high selectivity, *Talanta*, 2016, **148**, 229–236.
16. K. Prakash, P. R. Sahoo and S. Kumar, A substituted spiropyran for highly sensitive and selective colorimetric detection of cyanide ions, *Sens. Actuators, B*, 2016, **237**, 856–864.

17. S. Zhu, M. Li, L. Sheng, P. Chen, Y. Zhang and S. X. -A. Zhang, A spirooxazine derivative as a highly sensitive cyanide sensor by means of UV-visible difference spectroscopy, *Analyst*, 2012, **137**, 5581–5585.
18. A. K. Mahapatra, K. Maiti, S. K. Manna, R. Maji, C. D. Mukhopadhyay, B. Pakhira and S. Sarkar, Unique Fluorogenic Ratiometric Fluorescent Chemodosimeter for Rapid Sensing of CN^- in Water, *Chem. Asian J.*, 2014, **9**, 3623–3632.
19. A. Promchat, P. Rashatasakhon and M. Sukwattanasinitt, A novel indolium salt as a highly sensitive and selective fluorescent sensor for cyanide detection in water, *J. Haz. Chem.*, 2017, **329**, 255–261.
20. Y. Shiraishi, M. Itoh and T. Hirai, Colorimetric response of spiropyran derivative for anions in aqueous or organic media, *Tetrahedron*, 2011, **67**, 891–897.
21. Y. Yang, C. Yin, F. Huo, Y. Zhang and J. Chao, A ratiometric colorimetric and fluorescent chemosensor for rapid detection hydrogen sulfide and its bioimaging, *Sens. Actuators, B*, 2014, **203**, 596–601.
22. Y. Chen, C. Zhu, Z. Yang, J. Chen, Y. He, Y. Jiao, W. He, L. Qiu, J. Cen and Z. Guo, A Ratiometric Fluorescent Probe for Rapid Detection of Hydrogen Sulfide in Mitochondria, *Angew. Chem. Int. Ed. Engl.*, 2013, **52**, 1688–1691.
23. X. Feng, T. Zhang, J. -T. Liu, J. -Y. Miao and B. -X. Zhao, A new ratiometric fluorescent probe for rapid, sensitive and selective detection of endogenous hydrogen sulfide in mitochondria, *Chem. Commun.*, 2016, **52**, 3131–3134.
24. Q. Yu, K. Y. Zhang, H. Liang, Q. Zhao, T. Yang, S. Liu, C. Zhang, Z. Shi, W. Xu and W. Huang, Dual-Emissive Nanohybrid for Ratiometric Luminescence and Lifetime Imaging of Intracellular Hydrogen Sulfide, *ACS Appl. Mater. Interfaces*, 2015, **7**, 5462–5470.
25. A. Perry and D. Miles, An off-the-shelf sensor for colourimetric detection of sulfide, *Tetrahedron Lett.*, 2016, **57**, 5788–5793.
26. Y. Sun, S. Fan, S. Zhang, D. Zhao, L. Duan and R. Lia, A fluorescent turn-on probe based on benzo[e]indolium for bisulfite through 1,4-addition reaction, *Sens. Actuators, B*, 2014, **193**, 173–177.
27. M. Li, W. Feng, H. Zhang and G. Feng, An aza-coumarin-hemicyanine based near-infrared fluorescent probe for rapid, colorimetric and ratiometric detection of bisulfite in food and living cells, *Sens. Actuators, B*, 2017, **243**, 51–58.
28. W. -L. Wu, H. -L. Ma, M. -F. Huang, J. -Y. Miao and B. -X. Zhao, Mitochondria-targeted ratiometric fluorescent probe based on FRET for bisulfite, *Sens. Actuators, B*, 2017, **241**, 239–244.
29. Y. Li, Y. Duan, J. Li, J. Zheng, H. Yu and R. Yang, Simultaneous Nucleophilic-Substituted and Electrostatic Interactions for Thermal Switching of Spiropyran: A New Approach for Rapid and Selective Colorimetric Detection of Thiol-Containing Amino Acids, *Anal. Chem.*, 2012, **84**, 4732–4738.
30. Y. -H. Li, J. -F. Yang, C. -H. Liu, J. -S. Li and R. -H. Yang, Colorimetric and fluorescent detection of biological thiols in aqueous solution, *Chin. Chem. Lett.*, 2013, **24**, 96–98.
31. J. Liu, Y. -Q. Sun, Y. Huo, H. Zhang, L. Wang, P. Zhang, D. Song, Y. Shi and W. Guo, Simultaneous Fluorescence Sensing of Cys and GSH from Different Emission Channels, *J. Am. Chem. Soc.*, 2014, **136**, 574–577.

32. O. J. Cope and R. K. Brown, The Reduction of Nitrobenzene by Sodium Sulfide in Aqueous Ethanol, *Can. J. Chem.*, 1961, **39**, 1695–1710.
33. C. -M. Park, L. Weerasinghe, J. J. Day, J. M. Fukutob and M. Xian, Persulfides: current knowledge and challenges in chemistry and chemical biology, *Mol. BioSyst.*, 2015, **11**, 1775–1785.
34. S. Metsov, T. Dudev and V. Koleva, Infrared and NMR study of some 2-styrylindolium dyes, *J. Mol Struct.*, 1995, **350**, 241–246.
35. Q. Han, Z. Shi, X. Tang, L. Yang, Z. Mou, J. Li, J. Shi, C. Chen, W. Liu, H. Yang and W. Liu, A colorimetric and ratiometric fluorescent probe for distinguishing cysteine from biothiols in water and living cells, *Org. Biomol. Chem.*, 2014, **12**, 5023–5030.
36. X. Huang, X. Gu, G. Zhang and D. Zhang, A highly selective fluorescence turn-on detection of cyanide based on the aggregation of tetraphenylethylene molecules induced by chemical reaction, *Chem. Commun.*, 2012, **48**, 12195–12197.
37. M. Tomasulo, S. Sortino and F. M. Raymo, Bichromophoric Photochromes Based on the Opening and Closing of a Single Oxazine Ring, *J. Org. Chem.*, 2008, **73**, 118–126.
38. N. Karton-Lifshin, E. Segal, L. Omer, M. Portnoy, R. Satchi-Fainaro and D. Shabat, A Unique Paradigm for a Turn-ON Near-Infrared Cyanine-Based Probe: Noninvasive Intravital Optical Imaging of Hydrogen Peroxide, *J. Am. Chem. Soc.*, 2011, **133**, 10960–10965.
39. M. -Q. Wang, W. -X. Zhu, Z. -Z. Song, S. Li and Y. -Z. Zhang, A triphenylamine-based colorimetric and fluorescent probe with donor–bridge–acceptor structure for detection of G-quadruplex DNA, *Bioorg. Med. Chem. Lett.*, 2015, **25**, 5672–5676.
40. Y. Wang, I. Zhang, B. Yu, X. Fang, X. Su, Y. -M. Zhang, T. Zhang, B. Yang, M. Li and S. X. -A. Zhang, Full-color tunable mechanofluorochromism and excitation-dependent emissions of single-arm extended tetraphenylethylenes, *J. Mater. Chem. C*, 2015, **3**, 12328–12334.
41. R. G. Parr and R. G. Pearson, Absolute hardness: companion parameter to absolute electronegativity, *J. Am. Chem. Soc.*, 1983, **105**, 7512–7516.
42. J. -I. Fujisawa and M. Hanaya, Extremely strong organic–metal oxide electronic coupling caused by nucleophilic addition reaction, *Phys. Chem. Chem. Phys.*, 2015, **17**, 16285–16293.
43. S. C. George, S. Thulasi, S. Anas, K. V. Radhakrishnan and Y. Yamamoto, Palladium Catalyzed 1,8-Conjugate Addition to Heptafulvene via Bis-π-allyl Palladium Complexes, *Org. Lett.*, 2011, **13**, 4984–4987.
44. D. Huber, G. Andermann and G. Leclerc, Selective reduction of aromatic / aliphatic nitro groups by sodium sulfide, *Tetrahedron Lett.*, 1988, **29**, 635–638.
45. M. J. Frisch, G. W. Trucks, H. B. Schlegel, G. E. Scuseria, M. A. Robb, J. R. Cheeseman, G. Scalmani, V. Barone, G. A. Petersson, H. Nakatsuji, X. Li, M. Caricato, A. V. Marenich, J. Bloino, B. G. Janesko, R. Gomperts, B. Mennucci, H. P. Hratchian, J. V. Ortiz, A. F. Izmaylov, J. L. Sonnenberg, D. Williams-Young, F. Ding, F. Lipparini, F. Egidi, J. Goings, B. Peng, A. Petrone, T. Henderson, D. Ranasinghe, V. G. Zakrzewski, J. Gao, N. Rega, G. Zheng, W. Liang, M. Hada, M. Ehara, K. Toyota, R. Fukuda, J. Hasegawa, M. Ishida, T. Nakajima, Y. Honda, O. Kitao, H. Nakai, T. Vreven, K. Throssell, J. A. Montgomery, Jr., J. E. Peralta, F. Ogliaro, M. J. Bearpark, J. J. Heyd, E.

N. Brothers, K. N. Kudin, V. N. Staroverov, T. A. Keith, R. Kobayashi, J. Normand, K. Raghavachari, A. P. Rendell, J. C. Burant, S. S. Iyengar, J. Tomasi, M. Cossi, J. M. Millam, M. Klene, C. Adamo, R. Cammi, J. W. Ochterski, R. L. Martin, K. Morokuma, O. Farkas, J. B. Foresman and D. J. Fox, Gaussian 16 (Revision B.01), Gaussian Inc., Wallingford, CT, 2016.
46. E. I. Balmond, B. K. Tautges, A. L. Faulkner, V. W. Or, B. M. Hodur, J. T. Shaw and A. Y. Louie, Comparative Evaluation of Substituent Effect on the Photochromic Properties of Spiropyrans and Spirooxazines, *J. Org. Chem.*, 2016, **81**, 8744–8758.
47. K. Y. Ryu, T. G. Jo, D. Y. Park and C. Kim, Experimental and Theoretical Studies for the Recognition of Multiple Anions (Cyanide and Sulfide) Based on a Thiazole-Derived Chemosensor, *Sens. Lett.*, 2017, **15**, 111–125.